Synthesis and characterization of transparent Eu^{3+}:$LiNbO_3$ nanocrystalline glass-ceramics

QIONG SONG[a,b], YANKUI MIAO[c], CHUNHUI SU[a,d,*], HONGBO ZHANG[a,*], JING SHAO[a], XIAOWEI ZHU[b]
[a]*School of Material Science and Engineering, Changchun University of Science and Technology, Changchun-130022, China*
[b]*School of Food Engineering, Jilin Engineering Normal University, Changchun-130052, China*
[c]*BASF Shanghai Coatings Company Limited, Changchun 130000, PR China*
[d]*Changchun Normal University, Changchun-130032, China*

The glass-ceramics containing nanocrystalline lithiumniobate in the $38B_2O_3$-$30Nb_2O_5$-$15Li_2O$-$7KNO_3$-$5Sb_2O_3$-$5Eu_2O_3$(wt%) glass system were prepared by the melt-quench technique and controlling heat treatment. Samples were characterized by differential scanning calorimetry(DSC), X-ray diffraction(XRD), scanning electron microscope(SEM) and fluorescence spectrophotometer and the factors affecting the crystallization of glass-ceramics were analyzed. Scanning electron microscopy showed the fact that the $LiNbO_3$ nanocrystals dispersed in the glass matrix randomly. Fluorescence spectrum showed four emission peak, which located in the 578 nm ($^5D_0$-$^7F_0$), 592 nm ($^5D_0$-$^7F_1$), 615 nm ($^5D_0$-$^7F_2$) and 654 nm ($^5D_0$-$^7F_3$). The emission peak intensity of Eu^{3+} in the glass ceramic sample were greater than that in the parent glass. The luminescence spectra of Eu^{3+}-doped glass ceramics were recorded under 394 nm excitation and the luminescence intensity increase with the increasing of heat-treatment time. The optical transmittance reaches about 85% in visible light region. The Eu^{3+} -doped nanocrystalline $LiNbO_3$ glass–ceramics are promising candidate materials as red-light source due to the high luminescence intensity of Eu^{3+} at 592 nm and 615 nm.

(Received April 23, 2016; accepted August 9, 2017)

Keywords: Luminescence, Glass ceramics, Eu^{3+} -doped, Nanocrystalline $LiNbO_3$

1. Introduction

Glass ceramics are the glasses containing crystalline particles whose size is from nanometer to micrometer and have better properties than their parent glasses [1-3]. Glass ceramic is applied widely in capacitors and optoelectronic devices. Because it has a wide range of components and high dielectric constant [4–7]. Therefore, researchers focused on electrical properties for glass ceramic. In recent years, the researchers have reported the glass–ceramics doped with rare-earth (RE) ions containing $SrNbO_3$, $LiTaO_3$,$Y_3Al_5O_{12}$, $Bi_4Ti_3O_{12}$, and $ZnWO_4$ nanaocrystalline for their excellent optical properties [8–13]. In addition to these, the researchers focus on that how to improve the luminescence properties of RE-doped glass nanocomposites [14-17].

It is generally known that lithiumniobate ($LiNbO_3$) is superior ferroelectric material with the $A^{1+}B^{5+}O_3$ perovskite-type crystal structure. Lithiumniobate ceramic is applied in photonic and optoelectronic devices such as frequency doubling, tunable wave guiding, active laser host, holo-graphic storage and surface acoustic wave [18-19]. Lithiumniobate has showed an important value that it is promising candidate materials as lead-free piezoelectric ceramics material [20]. In recent years, The researchers are an increasing academic and technological interested in the research of glass ceramic containing lithiumniobate nannocrystalline, due to the glass ceramics have the advantages of low cost, high speed fabrication process, high doping concentration of rare earth, and controllable crystallization, compared to single crystal preparation. A large photoelectricity effect has been finded in a lot of transparent glass-ceramic materials [21].

In this study, the Eu^{3+} doped transparent glass-ceramic materials containing lithiumniobate nanocrystalline have been prepared by the approach of crystallization of glass and the luminescent properties of the samples were studied.

2. Experimental procedure

2.1. Preparation

The glass that the composition is $38B_2O_3$-$30Nb_2O_5$-$15Li_2O$-$7KNO_3$-$5Sb_2O_3$-$5Eu_2O_3$ (wt%) was prepared by melt-quench technique. The purity of the raw materials is 99.9%. The Sb_2O_3 is clarifying agent, it can exhibit eminent clarifying effect when it is used with together nitrate. The raw material was mixed thoroughly in an agate mortar and melted in a platinum crucible in an electric furnace at 1400℃ for 3 h in air with intermittent stirring for homogenization of the glass melt. The glass melt was poured onto a preheated mold made of cast iron,

followed by annealing at 480℃ for 2 h to remove the internal stresses in the glass, and then slowly cooled down to the room temperature. This glass is designated as precursor glass. Eu^{3+}-doped transparent glass-ceramics containing nanocrystalline $LiNbO_3$ was prepared by controlling heat treatment. The sample was cut into desired dimensions and for undertaking different experiments and measurements.

2.2. Characterization

Differential scanning calorimetry(DSC) and thermo-gravimetric analysis(TGA) measurements were carried out on a Netzsch STA 449 F3 instrument from the room temperature to 1000℃at a heating rate of 10 ℃ /min. The density(d) of as-prepared glass was determined at room temperature by the standard Archimedes principle using water as the buoyancy liquid. X-ray diffraction (XRD) data were recorded using an Rig aku D/max 2500V with the anchor scan parameters wavelength CuKa equal 1.5406×10^{-9}nm at 300 K, having a source power of 30 kV and 20mA, for identifying the developed crystalline phases of the heat-treated glass–ceramics. The nanocrystallinity of the heat-treated glasses was examined by the SEM.A Carl Zeiss high resolution Scanning Electron Microscope (SEM), model PHILIPS XL-30 detector (lithium doped silicon). Transmittance was examined by the UV - 3101 PC uv-visible near infrared spectrophotometer from shimadzu. Fluorescence spectrum of sample was recorded using a PL9000 fluorescence spectrometer from the BIO - RAD company, its Measuring range is 500 ~ 700 nm, scanning rate is 1200 nm/min, step length is 0.2 nm.

3. Results and discussion

3.1. DSC/TGA analysis and physical properties

The sample doped with 5.0 wt% Eu^{3+} was analyzed by DSC/TGA. The TGA measurement results show that the weight loss is less than 1% which value is in a limited range.

As shown in Fig. 1, the glass transition temperature(T_g) has been estimated from the intersection of the tangents drawn at the temperature that slope changed as 568℃ (Table 1). There are two exothermic peaks at 620℃(T1) and 770℃(T2) corresponding to the phase crystallization. The exothermic peak at 620 ℃ corresponds to the crystallization temperature region of LiNbO3 crystallites. From DSC curve, the ΔT(ΔT=T1-Tg) has been observed to be 60℃ and it represents the thermal stability of the glass. The glass-ceramics containing nanocrystalline lithiumniobate can be prepared by controlled heat-treatment due to the reasonably high glass stability factor [22]. The onset of crystallization temperature is 610℃. Crystal growth rate was the fastest at 620℃.

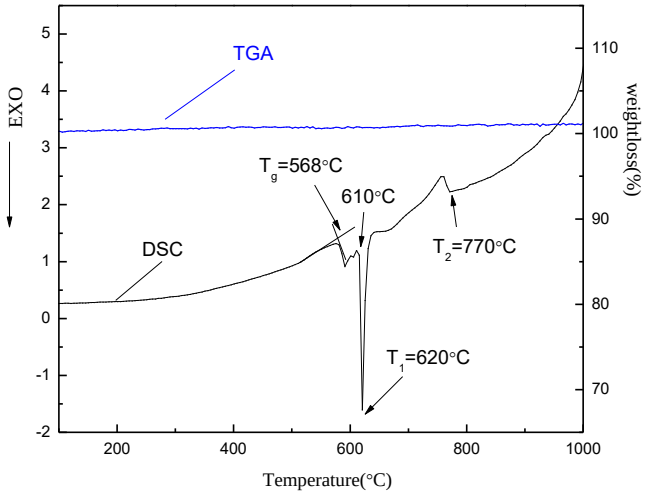

Fig. 1. Differential scanning calorimetry(DSC) and thermo-gravimetric analysis(TGA) of sample

Table 1. Physical Properties of as-prepared glass

Properties	Corresponding value
Glass transition temperature, T_g(℃)	568
Onset crystallization, T_o(℃)	610
First crystallization peak,T_1(℃)	620
Second crystallization peak,T_2(℃)	770
Average molecule weight, M_{av}(g/mol)	113.03
Density, ρ(g/cm^3)	3.465
Molar volume, V_m(cm^3/mol)	32.62

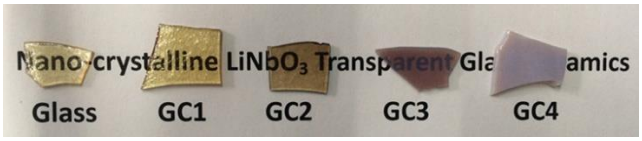

Fig. 2. Photograph of the precursor glass and glass-ceramics

Therefore, the temperature lower than the highest peak crystallization temperature was chosen for heat treatment to obtain transparent glass–ceramics and the crystallization behavior of the glass–ceramics are investigated. The samples were heat-treated at 625℃ for 1h, 2h, 3h, 4h and labeled as GC1, GC2, GC3, GC4, respectively. We see with the naked eye that the samples GC1 and GC2 are optical transparency, the sample GC3 is translucent and the sample GC4 is non-transparent. The transparency of the glass and glass-ceramics are shown in Fig. 2.

3.2. XRD analysis

The XRD pattern of the matrix glass is shown in Fig.

3(a). The XRD pattern of the matrix glass demonstrates no sharp peaks due to the amorphous nature of the matrix glass. The XRD patterns of heat-treated glasses at 625°Cfor 1h, 2h, 3h, 4h are shown in Fig. 3(b-e). The XRD spectrum of the sample diffraction peak consistent with JCPDS card of $LiNbO_3$(20-0631). The data revealed the appearance of this diffraction patterns due to the formation of $LiNbO_3$ crystals in the glass matrix. It is found there is no other crystal phase except $LiNbO_3$ when the matrix glass is doped with Eu^{3+}. It is well-known that niobium ions are highly oxidiz-able, therefore, the formation of $LiNbO_3$ crystal in the ambient conditions is difficult [23].

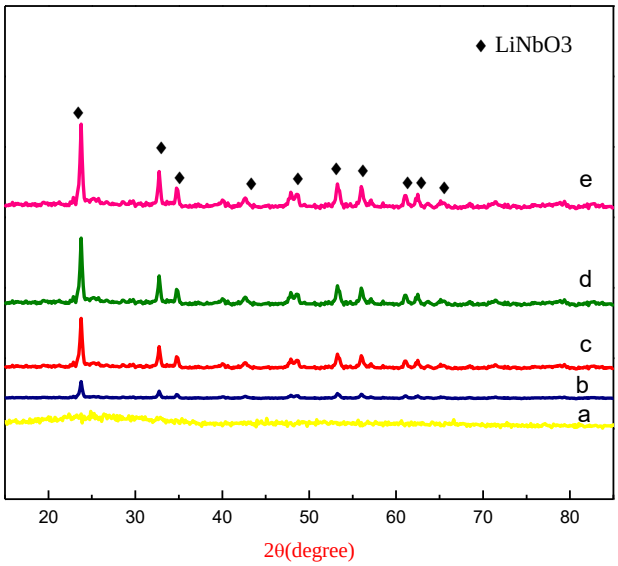

Fig. 3. XRD patterns of (a) the base glass; (b)GC1h;(c)GC2h;(d)GC3h;(e)GC4h

The average crystallite sizes(d) were calculated by using the Scherrer's formula.

$$D = \frac{k\lambda}{\beta cos\theta}$$

Where λ is the wavelength of X-ray radiation (Cu K a=1.5406 Å), β is the full width at half maximum (FWHM) of the peak at 2θ. K is Scherrer constant (k=0.89). The range of the average crystallite sizes calculated is 7–14 nm. As shown in Fig. 4, the size of crystalline increase with the increase of heat treatment time.

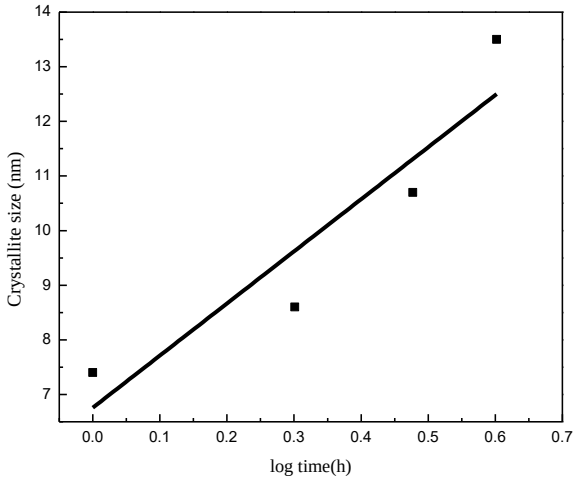

Fig. 4. Variation of crystallite size as obtained from XRD

3.3. SEM image analysis

Fig. 5(a)-(d) show that the SEM images of the samples that heat treated at 625°C for 1h, 2h, 3h and 4h,respectively. As shown in the SEM photo, it is clearly observed that the spherical crystallite was dispersed in the matrix glass. Because of the precipitation of crystal phase of the Li_2O-Nb_2O_5 system is constantly consumed doping components in the matrix glass with the growth of crystallite in all directions. Therefore, the energy of the Li_2O-Nb_2O_5 system is getting weaker and weaker with the growth of crystallite, and the end region of the crystallization is produced in the spherical surface, which leads to the formation of the globular crystal forming region. The particle size can be estimated to be about 60-80 nm from the SEM images. The crystalline size (7–14 nm) calculated from the XRD figures are lesser than that of the particle size estimated from the SEM (60–80nm), due to the fact that the relatively large size grains are surrounded by a number of smaller size grain, resulting in a large number of polygonal grains (grain edges Which is defined as the number of grains with different orientations in contact with each other), these polygonal grains gradually engulfed the surrounding small grains in the subsequent growth process, and the grain size difference becomes large [24, 25]. The precipitated phase of the system constantly depletes the dopant component of the matrix glass in the process of grain growth. The energy of the crystalline phase of the Li_2O-Nb_2O_5 system becomes weaker as the crystal grows, and the final crystallization region is formed [26].

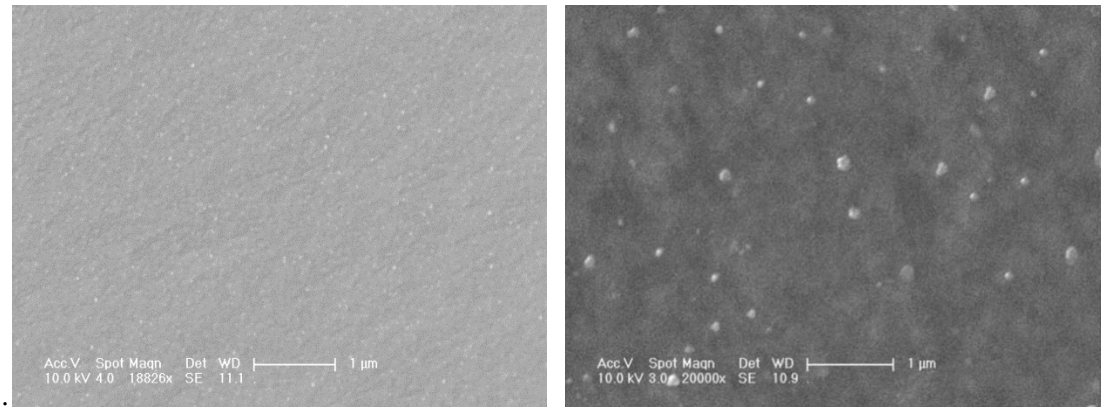

(a) GC1:625℃, 1h (b)GC2:625℃, 2h

(c) GC3:625℃, 3h (d)GC4:625℃, 4h

Fig. 5. SEM micrograph of heat-treated glasses at 625°C for1h,2h,3h,4h

3.4. Transmittance analysis

Fig. 6 shows the transmittance curve of the sample with 1 mm thickness at 625 ^{o}C for 1h, 2h, 3h and 4h. From the transmittance spectra, it is clearly observed that the gradual reduce of transmittance of the heat-treated samples with the increase of the heat-treatment time. Transmittance of the heat-treated samples at 625 ^{o}C for 1h is 85% and the transmittance is 60% if the heat treatment time is changed to 4h, due to the crystals grow more completely with the increase of the heat-treatment time. The increase of crystallite size enlarges refraction of light in the crystals, and also changes the distance between the crystal phase and glass phase, so the nonuniformity of structure was increased.

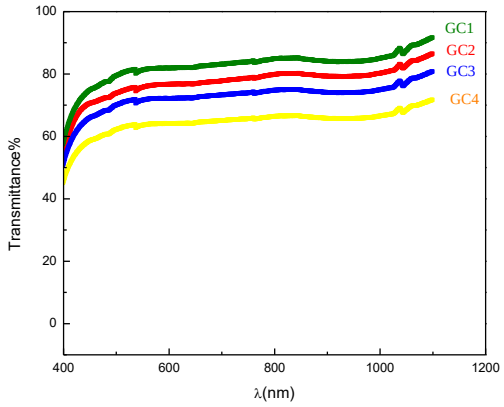

Fig. 6. Transmittance curve for sample

3.5. Luminescence spectra analysis

The emission spectra of the precursor glass and the glass–ceramics under the excitation at 394nm monochromatic light from a Xe lamp is shown in Fig. 7. Fig. 7 shows that fluorescence spectra has four luminescence bands. The spectra of the Eu^{3+}-doped glass and the glass–ceramics present four emission peaks at 578,

592, 613 and 653nm corresponding to the $^5D_0 \rightarrow {}^7F_0$, $^5D_0 \rightarrow {}^7F_1$, $^5D_0 \rightarrow {}^7F_2$, $^5D_0 \rightarrow {}^7F_3$ transition. The $^5D_0 \rightarrow {}^7F_1$ transition at 592 nm is the magnetcopy pole, and the change in the surrounding environment and structure of the ion does not change much about the intensity of the radiation. The $^5D_0 \rightarrow {}^7F_2$ transition of 613nm is an electric dipole, which is very sensitive to the change of the surrounding structure and is greatly influenced by the symmetrical center of Eu^{3+}. The structure of the interior of the crystal is regular and orderly, and the glass is amorphous, the internal arrangement is disordered and the energy dissipated in the glass is large, so the phonon energy is higher than that of the microcrystals. After the heat treatment, the local phonon energy of some Eu^{3+} decreases, which makes the multi - phonon relaxation probability smaller, the non - radiation transition decreases, the probability of radiation transition increases, and the fluorescence intensity increases [27, 28]. The red emission peak intensity increases with the increase in the heat-treatment time and reached maximum at four hours.

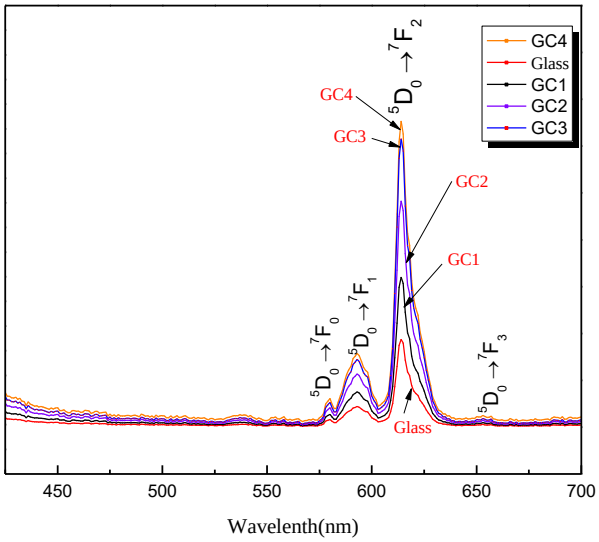

Fig. 7. Photoluminescence emission spectra of the sample

4. Conclusions

The Eu^{3+} doped transparent glass ceramic containing nanocrystalline $LiNbO_3$ have successfully been prepared in accordance with the composition of $38B_2O_3$-$30Nb_2O_5$-$15Li_2O$-$7KNO_3$-$5Sb_2O_3$-$5Eu_2O_3$ (wt%) by a melt quenching technique and then the matrix glasses are heat-treated at 625℃ for different times. The formation of nanocrystalline $LiNbO_3$ in the glass matrix was confirmed by the XRD, SEM. The size of crystalline determined by XRD is found to vary in the range of 7-14 nm. Fluorescence spectrum showed four emission peak which located at the 578 nm ($^5D_0$-$^7F_0$), 592 nm ($^5D_0$-$^7F_1$), 615 nm ($^5D_0$-$^7F_2$) and 654 nm ($^5D_0$-$^7F_3$), respectively. Eu^{3+} emission peak intensity in the glass ceramic samples were greater than the parent glass. The luminescence spectra of Eu^{3+}-doped glass–ceramics were recorded at 394 nm excitation wavelength and the luminescence intensity is found to be increased with the increase of heat-treatment time due to the increase of crystallinity. The optical transmittance reaches about 85% at 758 nm in visible light band. The high intensity ratio of $^5D_0$-$^7F_2$ to $^5D_0$-$^7F_1$ indicates that the Eu^{3+} -doped nanocrystalline $LiNbO_3$ glass–ceramics are promising candidate materials as red-light source.

Acknowledgements

The corresponding author of this paper is Chun-hui Su, Jing Shao. This work was financially supported by the National 863 Project (2011AA030204), Key Research Project of Jilin Provincial Science and Technology Department (20160204027GX).

References

[1] T. K. Yadav, A. K. Singh, K. Kumar, R. A. Yadav, Optical Materials **33**, 11 (2011).
[2] H. B. George, R. P. Linda, J. Am. Ceram. Soc. **82**, 9 (1999).
[3] C. Barry Carter, M. Grant Norton, Science and Engineering of Materials, Springer chp. 12, (2007).
[4] Upender Gangadharini, Atiar Rahaman Molla, Anal Tarafder, Basudeb Karmakar, J. Am. Ceram. Soc. **96**, 2155 (2013).
[5] A. Herczog, IEEE Trans. on Part H **9**(4), (1973).
[6] P. Gupta, H. Jain, D. B. Williams, O. Kanert, R. Kuechler, J. Non-Cryst. Solids **349**, 291 (2004).
[7] K. Narita, Y. Takahashi, Y. Benino, T. Fujiwara, T. Komatsu, Opt. Mater. **25**, 393 (2004).
[8] R. S. Chaliha, K. Annapurna, A. Tarafder, V. S. Tiwari, P. K. Gupta, B. Karmakar, Solid State Sciences **11**(8), 1325 (2009).
[9] A. Tarafder, K. Annapurna, R. S. Chaliha, V. S. Tiwari, P. K. Gupta, B. Karmakar, J. Alloy. Compd. **489**(1), 281 (2010).
[10] A. Tarafder, A. R. Molla, B. Karmakar, J. Am. Ceram. Soc. **93**, 1 (2010).
[11] A. R. Molla, A. Tarafder, B. Karmakar, J. Mater. Sci. **46**(9), 2967 (2011).
[12] R. K. Gupta, K. Ghosh, R. A. Patel, P. K. Kahol, Optoelectron. Adv. Mat. **2**(1), 12 (2008).
[13] V. Mehta, S. P. Singh, R. P. Chauhan, G. S. Mudahar, Optoelectron. Adv. Mat. **8**(9-10), 943 (2014).
[14] A. Tarafder, A. R. Molla, S. Mukhopadhyay, B. Karmakar, J. Am. Ceram. Soc. **95**(6), 1851 (2012).
[15] D. Ridgley, R. Ward, J. Am. Chem. Soc. **77**(23), 6132 (1955).
[16] E. I. Krylov, A. A. Sharnin, J. Gen. Chem. **25**, 1345 (1955).
[17] I. A. Leonidov, V. L. Kozhevnikov, E. B. Mitberg, M. V. Patrakeev, V. V. Kharton, F. M. B. Marques, J. Mater. Chem. **11**(4), 1201 (2001).
[18] V. V. Kharton, A. V. Kovalevsky, A. P. Viskup, J. R. Jurado, F. M. Figueiredo, E. N. Naumovich, J. R. Frade, J. Solid State Chem. **156**(2), 437 (2001).

[19] M. Zgonik, R. Schlesser, I. Biaggio, E. Voit, J. Tscherry, P. Giinter, J. Appl. Physiol. **74**, 1893 (1993).
[20] D. F. Xue, S. Y. Zhang, Chem. Phys. Lett. **54**, 401 (1998).
[21] E. Ringgaard, T. Wurlitzer, J. Eur. Ceram. Soc. **25**, 2701 (2005).
[22] Reenamoni Saikia Chalihaa, K. Annapurna, Anal Tarafder, V. S. Tiwari, Solid State Science **11**, (2009).
[23] N. H. Peng, J. T. S. Irvine, A. G. Fitzgerald, J. Mater. Chem. **8**, 1033 (1998).
[24] Reenamoni Saikia Chalihaa, K. Annapurnaa, Anal Tarafdera, V. S. Tiwarib, Optical Materials **32**, (2010).
[25] H. Tanaka, M. Yamamoto, Y. Takahashi, Y. Benino, T. Fujiwara, T. Komatsu, Opt. Mater. **22**, 71 (2003).
[26] B. Sumuneva, St. Sumuneva, V. Dimitrov, J. Non-Cryst. Solids **129**, 54 (1991).
[27] C. H. Kam, S. Buddhudu, Journal of Quantitative Spectroscopy & Radiative Transfer **87**, 325 (2004).
[28] D. Chen, Y. Yu, P. Huang, H. Lin, Z. Shan, Y. Wang, Acta Mater. **58**, 3035 (2010).

*Corresponding author: sch@cust.edu.cn
zhb5388460@126.com